RESEARCH ARTICLE | OCTOBER 18 2024

# Thermodynamic temperatures of Fe-C, Pd-C, Ru-C and WC-C for the *Mise-en-Pratique* of the Kelvin up to 3020 K

M. Sadli ≤; F. Bourson; D. Lowe; K. Anhalt; D. Taubert; M. J. Martin; J. M. Mantilla; F. Girard; M. Florio; C. Gözönünde; H. Nasibli; L. Kňazovická; N. Sasajima; X. Lu; O. Kozlova; S. Briaudeau; G. Machin

AIP Conf. Proc. 3230, 020004 (2024) https://doi.org/10.1063/5.0234550





# Articles You May Be Interested In

Realizing the redefined Kelvin: Realization and dissemination of the Kelvin below 25 K

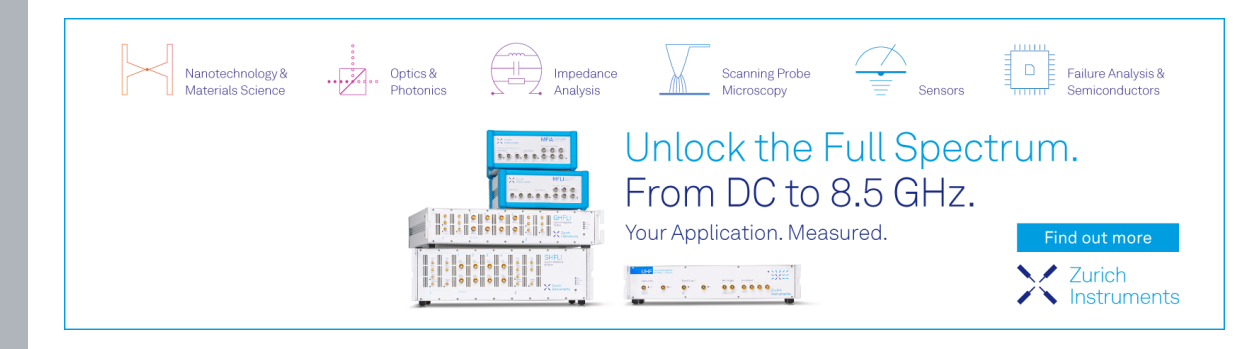
AIP Conf. Proc. (October 2024)

Realizing the redefined Kelvin: Extending the life of ITS-90

AIP Conf. Proc. (October 2024)

Future of the international temperature scale in a mixed dissemination environment

AIP Conf. Proc. (October 2024)





# Thermodynamic Temperatures of Fe-C, Pd-C, Ru-C and WC-C for the *Mise-en-Pratique* of the Kelvin up to 3020 K

M. Sadli<sup>1, a)</sup>, F. Bourson<sup>1</sup>, D. Lowe<sup>2</sup>, K. Anhalt<sup>3</sup>, D. Taubert<sup>3</sup>, M.J. Martin<sup>4</sup>, J.M. Mantilla<sup>4</sup>, F. Girard<sup>5</sup>, M. Florio<sup>5</sup>, C. Gözönünde<sup>6</sup>, H. Nasibli<sup>6</sup>, L. Kňazovická<sup>7</sup>, N. Sasajima<sup>8</sup>, X. Lu<sup>9</sup>, O. Kozlova<sup>1</sup>, S. Briaudeau<sup>1</sup>, and G. Machin<sup>2</sup>

<sup>1</sup>LNE-Cnam Laboratoire commun de métrologie, Saint Denis, France

<sup>2</sup>NPL National Physical Laboratory, Teddington, UK

<sup>3</sup>PTB, Physikalisch-Technische Bundesanstalt, Berlin, Germany

<sup>4</sup>CEM, Centro Español de Metrología, Tres Cantos, Spain

<sup>5</sup>Istituto Nazionale di Ricerca Metrologica, Turin, Italy

<sup>6</sup>TUBITAK-UME, Gebze, Türkiye

<sup>7</sup>CMI, Czech Metrology Institute, Brno, Czech Republic

<sup>8</sup>NMIJ, National Metrology Institute of Japan, Tsukuba, Japan

<sup>9</sup>NIM, National Institute of Metrology, Beijing, People's Republic of China

a)Corresponding author: mohamed.sadli@lecnam.net

**Abstract.** The *Mise-en-Pratique* for the definition of the kelvin at high temperatures has opened the possibility of disseminating thermodynamic temperature through relative primary radiometry mediated by high-temperature fixed points (HTFPs). The thermodynamic temperatures of Co-C, Pt-C and Re-C were assigned in 2016. Here, we report on the assignment of thermodynamic temperatures of the phase transitions of four more HTFPs, namely, Fe-C ~1427 K, Pd-C ~1765 K, Ru-C ~2227 K and WC-C ~3021 K, with expanded uncertainties ranging from 0.15 K to 0.27 K.

#### INTRODUCTION

The high-temperature range, above 1000 °C, is one of the ranges in which the redefinition of the kelvin may have the most promising possibilities. We have known for a couple of decades that thermodynamic temperature obtained by radiometric methods with a direct traceability to the cryogenic radiometer could compete with ITS-90 scheme above 1800 K. The main reason why ITS-90 persists as the main approach to realising and disseminating the kelvin above the silver point is that it is easy to set up and maintain, at least compared to absolute primary radiometry. However, it is clear that using absolute primary radiometry, through filter radiometers and filter or grating-based spectroradiometers, radiometric temperature measurements at the level of a few 10<sup>-4</sup> in terms of radiance can be achieved. The first measurements of the thermodynamic temperatures of high-temperature fixed points were performed in 2005 and the uncertainties and the comparability of the cells were already at a relatively good level [1]. At that moment, the quality of the high-temperature fixed point (HTFP) cells was not optimal, and the implementation methods needed to be improved, for example to consider the thermal effects of the furnaces.

Ten years later, following thorough research in several NMIs [2], especially for studying the thermal effects [3] and for improving the design of the cells and the filling processes [4], three HTFPs: Co-C, Pt-C and Re-C, were available in sufficiently high purity grade metal (99.99 % purity or better) and were widely characterised and identified as the most promising HTFPs for the assignment of thermodynamic temperature. This was successfully done in 2015 in the frame of the EURAMET-funded joint research project "Implementing the new kelvin" [5]. The thermodynamic temperature of the phase transition of these three HTFPs, as well as the copper point, were determined by a consortium of 9 NMIs/DIs. The liquidus temperature [6] and the point-of-inflection of the melting plateau (POI in this document)

temperature [7] were determined collectively with unprecedented uncertainty levels impossible to achieve by a single NMI.

Consequently, a task group of the CCT working group "non-contact thermometry" identified the uncertainties which needed to be considered when using these HTFPs as thermodynamic temperature references [8].

More widely, and in the context of the redefinition of the SI, the thermometry community paved the way to the *Mise-en-Pratique* of the new definition of the kelvin which was officially announced in May 2019. This *Mise-en-Pratique* included a high-temperature part in which relative primary thermometry mediated by high-temperature fixed points of assigned thermodynamic temperatures was recognised as an acceptable way for realising the new definition of the kelvin [9].

Shortly after the redefinition of the kelvin a joint research project "Realising the Redefined Kelvin (Real-K) [10], was initiated. This project covered a very wide temperature range from below 1 K to above 3000 K. The high-temperature part of the project had the following main objectives:

- Extend the temperature range of HTFPs to 3020 K by including work on the WC-C peritectic point.
- Bridge the gap between Cu, Co-C, Pt-C and Re-C by introducing the HTFPs of Fe-C, Pd-C, Ru-C.
- Prepare and anticipate the use of HTFPs with assigned thermodynamic temperatures to calibrate noble metal thermocouples (Pt/Pd for example) using Cu, Fe-C, Co-C and Pd-C.

To achieve these objectives, four-high temperature fixed points, namely Fe-C, Pd-C, Ru-C and WC-C, were selected and several participating institutes supplied HTFP cells for the temperature assignment process or for dissemination trials purposes. More than 28 HTFP cells were constructed for this project.

These HTFP cells were first characterised by their supplying institutes and their sensitivity to changing thermal conditions assessed according to a common protocol. The outcome of this study aimed at determining the thermal-related uncertainties is presented in [11].

In the following sections, the selection of the HTFP cells for thermodynamic temperature assignment, their initial and final comparison to assess their drift, and the results of the determination of the thermodynamic temperatures of the phase transitions (at the POI and at the liquidus point) will be presented and discussed.

#### SELECTION OF THE HTFP CELLS

A total of 28 HTFP cells were used in this project: 7 Fe-C, 6 Pd-C, 8 Ru-C and 7 WC-C. Most of them were already constructed at the beginning of the project. Almost all these cells showed good reproducibility levels and melting plateau shapes and underwent a selection process to identify the best ones to be used for the assignment of thermodynamic temperature.

The selection protocol, consisting of cell comparison, was based on that of the EURAMET project InK [5]. The main selection criteria were the melting temperature (the higher the better, assuming impurity would mainly decrease the phase transition temperature), the plateau shape, the melting range (the smaller the better, assuming that a small melting range would mean low concentrations of impurities) and the repeatability. At the end of the project, the selected cells were compared once again to check for any possible drift due to their intensive use.

Table 1 shows the laboratories which performed the initial comparison and those which performed the final comparison after the thermodynamic temperature measurements were completed by all the participants. It also shows the ranking of the cells; it was agreed that the best two cells would be used for thermodynamic temperature assignment while the third and fourth cells of Pd-C and Fe-C would be used for dissemination purposes [12].

# Properties of the cells

The HTFP cells involved in the comparison were all based on the hybrid design [13]. They were filled by incremental filling, or by the piston method, or both simultaneously. Table 2 shows the main properties of the cells selected for the comparison.

As can be seen in this table, the HTFP cells had different cavity dimensions so corrections for emissivity and temperature drop were applied to the thermodynamic temperature data to derive the phase transition temperatures.

**TABLE 1.** Laboratories involved in the cell comparison and cell ranking.

HTFP	Fe-C	Pd-C	Ru-C	WC-C
Initial comparison	INRIM	CEM	NPL	LNE-Cnam
Ranking 1st	1Fe-C4 (CEM)	7ST-5 (NMIJ)	Ru-C6 (VNIIOFI)	7WC-C3 (LNE-Cnam)
Ranking 2 <sup>nd</sup>	Fe-C1 (PTB)	XL17 (NIM)	Ru2001 (NPL)	7WC-C5 (LNE-Cnam)
Ranking 3 <sup>rd</sup>	Fe-C2 (PTB)	1Pd-C3 (CEM)	Ru-C7 (VNIIOFI)	7WC-C4 (LNE-Cnam)
Ranking 4th	1Fe-C2 (CEM)	DW12 (NIM)	7ST-9 (NMIJ)	WCC2004 (NPL)
Final comparison	LNE-Cnam	CEM	NPL	LNE-Cnam

**TABLE 2.** Properties of the cells selected for the thermodynamic temperature assignment process.

Cell ID	Cell diameter (mm)	Cell length (mm)	Cavity diameter (mm)	Cavity length (mm)	Mass of ingot (g)	Volume of the ingot (cm³)	Metal supplier	Nominal purity of the metal (ppm)
Fe-C1	24	45	3	31	28.7	4.08	Evochem	100
1Fe-C4	24	45	3	35	31.1	4.35	Sigma Aldrich	100
7Fe-C2*	24	44	3	34	26.7	3.82	Nippon Mining and metal	10
7ST-5 (Pd-C	) 24	45	3	34	27.3	2.7	Ishifuku	30
XL17 (Pd-C)	) 25	45	6	33	43	4.2	Alfa Aesar	100
Ru-C6	24	44.5	3	34	31.9	3.8	Furuya Metal Co.,	10
Ru2001	24	43	3	30	33.2	2.7	Furuya Metal Co.,	10
7WC-C3	24	44	3	34	60.8	3.82	Alfa Aesar	10
7WC-C5	24	44	3	34	57.7	3.82	Alfa Aesar	10

<sup>\*7</sup>Fe-C2 was not selected after the first comparison but showed significantly better performances at the final comparison and was taken as the reference cell for the assignment of thermodynamic temperature.

# INITIAL COMPARISON OF THE HTFP CELLS

## Fe-C fixed point

The initial comparison of the Fe-C HTFP was performed by INRIM with a home-made standard radiation thermometer of central wavelength 900 nm and a target field stop of 1.6 mm. Its day-to-day stability was monitored using a Cu fixed point. The Fe-C HTFPs were implemented in a 3-zone furnace which had a temperature distribution of about  $\pm$  0.1 K along the cell. Table 3 shows the cell evaluation data. The repeatability is assessed from the standard deviation of the temperature at the POI measured at different setpoints.

Note that Fe-C1 (PTB) was initially selected but was changed, by error, to 1Fe-C2 (CEM) during the circulation of the cells for the thermodynamic temperature assignment. So finally, cells 1Fe-C2 and 1Fe-C4, very close in terms of melting temperatures, were the two cells which circulated among the participants for the thermodynamic temperature assignment.

The plateau shape is an important indicator of the quality of the cells and their correct positioning in the furnace [3]. It is a criterion of selection even though it can be subjective. A good plateau would have a clear entrance in the plateau and a sharp run-off, exhibit a small melting range and should not show any irregularities.

**TABLE 3.** Properties of the Fe-C HTFP cells selected for the comparison.

Supplier		CEM		P	ГВ	LNE-	Cnam
Cell ID	1Fe-C2	1Fe-C3	1Fe-C4	Fe-C1	Fe-C2	7Fe-C1	7Fe-C2
Repeatability (mK)	6	9	7	6	12	6	12
Melting range (mK)	320	460	310	190	180	180	210
Difference to $T_{max}^{1}$ (mK)	-13	NA*	0	-2	-7	-29	-48
Plateau shape	Good	Short	Good	Best	Best	Poor	Poor
Ranking	4	NA*	1	2	3	5	6

<sup>\*</sup>NA: not applicable (in this case, the cell was used for dissemination trials [12]).

# **Pd-C** fixed point

The initial comparison of Pd-C HTFP was performed by CEM. A KE linearpyrometer LP4 at 650 nm central wavelength was used as the standard radiation thermometer. Its day-to-day stability was monitored using a Cu fixed point. The Pd-C HTFPs were implemented in a CHINO single zone furnace, model IR-R80. Table 4 shows the cell comparison results. The repeatability is assessed from the standard deviation of the temperature at the POI measured at different setpoints.

**TABLE 4.** Results of the Pd-C HTFP cell selection performed at CEM.

Supplier	CI	EM	NI	M	NMIJ
Cell ID	1Pd-C1	1Pd-C3	DW12	XL17	7ST-5
Repeatability (mK)	10	50	20	10	20
Melting range (mK)	500	490	360	300	230
Difference to T <sub>max</sub> (mK)	- 190	-120	-190	-70	0
Plateau shape	Good	Good	Good	Good	Good
Ranking	5	3	4	2	1

The two Pd-C cells selected for thermodynamic temperature assignment were therefore the cells 7ST-5 (NMIJ) and the cell XL17 (NIM).

# **Ru-C** fixed point

The initial comparison of Ru-C HTFP was performed by NPL. A KE LP3 linearpyrometer at 650 nm central wavelength was used as the standard radiation thermometer. Its day-to-day stability was monitored using a Cu fixed point. The Ru-C HTFPs were implemented in a CHINO single zone furnace, model IR-R80.

Table 5 shows the cell comparison results. The repeatability is assessed from the standard deviation of the temperature at the POI measured at different setpoints. The two cells which were selected were Ru-C6 and Ru2001.

<sup>&</sup>lt;sup>1</sup> Throughout tables 3 to 9, *Difference to T\_{max}* means the difference in the POI temperature for a given cell compared to the cell with the highest POI temperature.

**TABLE 5.** Results of the Ru-C HTFP cell selection performed at NPL.

Supplier	VNIIOFI		N	NPL		
Cell ID	Ru-C6	Ru-C7	Ru2001	Ru2002	7ST-9	
Repeatability (mK)	4	7	9	11	12	
Melting range (mK)	136	172	211	898	308	
Difference to $T_{max}$ (mK)	0	-69	-127	-647	-153	
Plateau shape	Very Good	Very Good	Good	Good	Good	
Ranking	1	3	2	5	4	

# WC-C fixed point

The initial comparison of the WC-C HTFP was performed by LNE-Cnam. A KE LP5 at 650 nm central wavelength was used as the standard radiation thermometer. Its day-to-day stability was monitored using a Cu fixed point. The WC-C HTFPs were implemented in a Vega HTBB 3200-PG single-zone furnace.

Table 6 shows the cell comparison results. The repeatability is derived from the standard deviation of the temperature at the POI measured with different setpoints.

**Supplier** LNE-Cnam NPL Cell ID 7WC-C3 7WC-C4 7WC-C5 WCC2003 WCC2004 5 Repeatability (mK) 17 15 11 10 195 Melting range (mK) 120 130 130 170 Difference to T<sub>max</sub> (mK) 0 -145 -52 -287 -227 Plateau shape Very good Good Very good Very good Good

3

**TABLE 6.** Results of the WC-C HTFP cell selection performed at LNE-Cnam.

# THERMODYNAMIC TEMPERATURE MEASUREMENTS

2

5

4

Once the cells had been compared and ranked, the best two cells of each batch were selected for circulation among the participating institutes in two loops for thermodynamic temperature assignment:

# Loop A:

Ranking

• Foreseen participants and circulation order: CEM, PTB, LNE-Cnam and NPL.

1

• Circulating cells: Fe-C 1Fe-C2(CEM); Pd-C 7ST-5 (NMIJ); Ru-C Ru-C6 (VNIIOFI); WC-C 7WC-C3 (LNE-Cnam).

#### Loop B:

- Foreseen participants and circulation order: VNIIOFI, UME, NIM and INRIM.
- Circulating cells: Fe-C 1Fe-C4 (CEM); Pd-C XL-17 (NIM); Ru-C RU2001 (NPL); WC-C 7WC-C5 (LNE-Cnam).

Note that the results from VNIIOFI have not been used in this study. Moreover, INRIM could not perform the measurements as planned due to delays in loop B with the measurement slot for INRIM moved to coincide with laboratory renovation works. Consequently, INRIM were unable to carry out the thermodynamic temperature measurements.

It is also important to note that the Fe-C cell selected in the initial comparison of cells as well as the contradictory results obtained at this point in the post measurement comparison campaign meant that a correction had to be applied to the Fe-C HTFP to derive the best estimate of the liquid-solid transition temperature.

In the section that follows a brief overview is given of the thermodynamic temperature measurement method applied by each participant. A protocol for the measurements was established and agreed by all participants prior to the start of the measurements. This protocol included, in particular, a sequence of melt/freeze temperature steps ranging from +15 K to +30 K for the melt initiation and -15 K to -40 K for the freeze initiation, over two days, for each HTFP.

The freezing temperatures were not considered in this work. The participants reported the thermodynamic temperatures at the POI of the melting plateau and at the liquidus point.

# Thermodynamic temperature measurements at CEM

Thermodynamic temperature measurement of the circulating HTFP cells was made with a KE linearpyrometer LP4 standard radiation thermometer, with an interference filter at the central wavelength of 650 nm. The LP4 can be calibrated in two ways to provide thermodynamic temperature:

- in absolute spectral responsivity, as explained in [14] (absolute primary radiometric thermometry)
- with reference to the CEM Cu fixed point (FP), with assigned T =  $(1357.78 \pm 0.21)$  K (k = 2) (relative primary radiometric thermometry)

The thermodynamic temperature of the CEM Cu fixed point was assigned prior to this measurement campaign using an LP4 calibrated in absolute spectral responsivity mode. Eventually the calculation of the thermodynamic temperature of the cells in this project was made using relative primary radiometric thermometry.

The Ru-C, Pd-C and Fe-C HTFP cells were installed in an IR-R80 CHINO furnace. The WC-C HTFP cell were installed in an Ultratherm BB3200M high temperature furnace.

All the HTFP cells were placed in the most homogeneous part of the furnace. This place was determined previously using CEM HTFP cells: the optimal placement was identified as the one where the melting plateaus lasted the longest and their ending was the sharpest.

The LP4 pyrometer was checked for drift by repeated Cu fixed point measurements on a weekly basis.

In addition, results from the Fe-C and Pd-C HTFP cells could be compared to the previous measurements of thermodynamic temperatures at these points. The differences between the relative and absolute thermodynamic temperature measurements [15], were much smaller than the combined uncertainties.

Corrections for the emissivity of the HTFP cells (with  $\epsilon$  = 0.9997 calculated with STEEP3® for the CEM Fe-C HTFP cell [and considered the same for the others]) and temperature drop were performed to derive the thermodynamic temperatures of the phase transitions.

#### Thermodynamic temperature measurements at PTB

PTB used the two-step radiance/irradiance comparison method described in [16]. Two high-temperature furnace systems were used: one which holds the HTFP cell (Chino type / Nagano M) and a second (HTBB 3200 pg) which acts as a reference source of thermal radiation.

The thermodynamic temperature of the reference source was determined by a direct spectral irradiance measurement with an absolutely-calibrated interference filter radiometer. The thermodynamic temperature of the HTFP during the melt could then be derived from a ratio measurement of spectral radiance between the HTFP and the HTBB.

The radiometer used for the radiance comparison was an IKE LP5 radiation thermometer with an effective wavelength of around 650 nm. A correction for the effect of the different geometry in radiance and irradiance mode was applied.

For the radiance measurement at the HTFP the LP5 was repositioned in front of the Nagano M furnace at a distance of 700 mm from the aperture of the HTFP cell and aligned to the center of this aperture. Corrections of emissivity of HTFP cells (with  $\varepsilon = 0.9997$ ), and temperature drop were performed to derive the thermodynamic temperatures of the phase transitions.

# Thermodynamic temperature measurements at NPL

NPL used two different furnaces for the implementation of the HTFP cells. The Chino IR-R80 furnace for Fe-C, Pd-C and Ru-C points and the Thermogauge furnace for WC-C point. The optimal position of the cells was determined from the results of the thermal effect study performed during this project [11].

The method used for the thermodynamic temperature determination uses the Cu point and the Re-C point with published values [5, 6] and the n = 2 model [17] using an LP5 (KE linearpyrometer) with a 650 nm filter of a bandwidth of 10 nm. The stability of the pyrometer was monitored by repeated measurements at the Cu and Re-C points and was estimated to be better than 27 mK at the Re-C point.

The reported temperature values were all corrected for emissivity and temperature drop to derive the phase transition thermodynamic temperatures.

# Thermodynamic temperature measurements at LNE-Cnam

LNE-Cnam uses the radiance method for the direct determination of thermodynamic temperature [18] using a radiance comparator to transfer the absolute radiance measurement performed with a radiancemeter to the HTFP cell. This method was applied to the Cu point and the WC-C point prior to the measurement campaign in this project. A relative method by extrapolation from the copper freezing point with the LNE-Cnam assigned thermodynamic temperature was applied with the classical ITS-90 extrapolation scheme using the radiance comparator [19]. The comparator was operated at the wavelength of 808 nm. To validate the relative method, the WC-C point was measured, and the determined thermodynamic temperature value was compared to the direct thermodynamic temperature measurement performed on a similar cell (constructed at LNE-Cnam with a different metal supplier for tungsten). A difference of less than 250 mK, determined with an uncertainty of about 1 K (k = 2), was obtained allowing the use of the relative method for the sake of simplicity.

The cells were implemented in the HTBB 3200 PG furnace in the most uniform zone of the furnace. The optimum positions of the HTFP cells were determined prior to the measurement campaign from the thermal effect studies performed in the second task of this project [11] using the methods developed at LNE-Cnam [3].

The reported temperature values were all corrected for emissivity and temperature drop to derive the phase transition thermodynamic temperatures.

#### Thermodynamic temperature measurements at NIM

Measurement at NIM on the HTFPs of Fe-C, Pd-C and Ru-C were made by the relative method based on the calibration of a linearpyrometer LP4 at the points of Cu, Co-C, Pt-C and Re-C with locally assigned thermodynamic temperatures reported in the InK project [5-7]. The LP4 had a 650 nm filter of a bandwidth of 10 nm. An interpolation scheme was applied and the temperatures of the phase transitions of the circulating HTFP cells were determined.

For the highest temperatures, the Ru-C and WC-C points were compared to NIM Ru-C and WC-C HTFP cells whose thermodynamic temperatures were determined in 2021 by a direct radiance-mode thermodynamic temperature measurement method. The differences between these cells allowed the assignment of thermodynamic temperature values.

It is worth noting that the Ru-C circulating cell was measured by both methods. The difference between the two determinations was less than 20 mK giving confidence in the equivalence of both approaches.

#### Thermodynamic temperature measurements at UME

Measurements at TUBITAK were performed using an LP5 pyrometer with a 650 nm interference filter with a spectral bandwidth of about 12 nm. The pyrometer was calibrated at the Cu point, and the Co-C and Re-C HTFPs, and an interpolation/extrapolation equation was derived with n = 1, 2 or 3 cases for the determination of the thermodynamic temperature of the circulating HTFPs.

The HTFP cells were implemented in an HTBB 3500 MM high-temperature furnace. Prior to the measurement campaign, an optimum position for each cell was determined using an iterative method, i.e. by shifting the cell location

inside the furnace to obtain a melting plateau with the longest duration and sharpest entering and exiting the melt. A dedicated three-zone furnace and a copper point cell were used to assess the LP5 pyrometer stability during the measurements. This was checked weekly during the measurements and before the start of measurements.

Along with the temperature drop correction, an emissivity correction with a value of 0.9997 was applied to retrieve the thermodynamic temperatures of the phase transitions.

#### FINAL CELL COMPARISON

# Fe-C fixed point

The final comparison of Fe-C HTFP cells was performed by LNE-Cnam using the pyrometer LP5 (650 nm) whose stability was daily monitored at the copper point. The cells were implemented in the HTBB 3200 PG furnace in the best temperature profile determined prior to the cell comparison process. The conditions of the comparison at LNE-Cnam were different from the initial comparison at INRIM where the furnace used was a three-zone furnace with a much larger thermal inertia. Moreover, Fe-C is a HTFP for which the thermal history has a proven effect on the phase transition temperature due to its structure [20].

The results of the final comparison were therefore quite different from the initial comparison at this point. They show a significant drift of the cells or a different behaviour of the cells in different furnaces. Table 7 shows the results of the final comparison in which the LNE-Cnam cells were finally ranked first and second. At least one of these cells was intensively used during the project for the determination of the thermal effects [11] and it was still very close to the other cell constructed by LNE-Cnam. This was not a surprise as the metal used in these cells was of a better nominal purity (5N) than the other cells of the project.

In conclusion, the assigned temperature was corrected to take the final temperature differences between cells into account (0.20 K correction at the POI and 0.16 K at the liquidus point) and a standard uncertainty of 58 mK (200 mK /  $2\sqrt{3}$ ) was added to the uncertainty of determination of the thermodynamic temperature value to account for the drift and the difference between the circulating cell and the reference cell.

**TABLE 7.** Results of the final comparison of the Fe-C HTFP cells at LNE-Cnam. The two HTFP cells which circulated for thermodynamic temperature assignment are underlined.

Supplier	CEM		P	ГВ	LNE-	LNE-Cnam	
Cell ID	<u>1Fe-C2</u>	1FeC4	Fe-C1	Fe-C2	7Fe-C1	7Fe-C2	
Repeatability (mK)	30	29	20	17	9	19	
Melting range (mK)	650	550	300	310	300	280	
Difference to $T_{max}$ (mK)	-200	-190	-120	-230	-25	0	
Plateau shape	Poor	Poor	Good	Good	Good	Good	

## **Pd-C** fixed point

The final comparison of Pd-C HTFP cells was performed by CEM, as for the initial comparison, using the pyrometer LP4 (650 nm). The measurements were performed with each cell installed in the Chino IR-80 furnace in its most uniform zone. Results reported in table 8 correspond to the averages of two days of measurements in the aforementioned position.

These results show that the two cells ranked first and second after the first comparison of the cells were still the best after their circulation. The cell DW12 was broken during the thermal effect determination at CMI and is not presented in this table.

**TABLE 8.** Results of the initial (2021) and final (2023) measurements on the Pd-C cells at CEM. The two HTFP cells which circulated for thermodynamic temperature assignment are underlined.

Supplier	CEM		NIM	NMIJ
Cell ID	1Pd-C1	1Pd-C3	<u>XL17</u>	<u>7ST-5</u>
Initial POI (2021) (K)	1765.12	1765.18	1765.23	1765.31
Final POI (2023) (K)	1764.81	1765.06	1765.19	1765.23
Difference to T <sub>max</sub> (2023) (mK)	-340	-170	-40	0
Drift (2023-2021) (mK)	-310	-120	-40	-80
Plateau shape (2023)	Poor	Poor	Good	Good

A drift of 40 mK and 80 mK was noticed on the ITS-90 temperature measurements of the cells XL17 and 7ST-5. The uncertainty on these values corresponds to the ITS-90 realisation uncertainty at CEM with the LP4 which is 380 mK (k=2). Therefore, the cells will be considered as stable and no correction for drift will be applied. However, a standard uncertainty of 24 mK (80 mK /  $2\sqrt{3}$ ) was added to the uncertainty budget to account for the effect the observed drift and the difference between the circulating cells on this result.

# Ru-C fixed point

The final comparison of Ru-C HTFP cells was performed by NPL, as per the initial comparison, using the same means and protocol as the initial comparison. The measurements were performed with each fixed-point cell installed in the Chino IR-80 furnace and the temperature of each cell was measured. The results are given in table 9. They show the thermodynamic temperature results of the cells obtained during the initial comparison and the final comparison of the cells. The cell RU2002 was taken as a reference since it remained unused during the whole duration of the project.

**TABLE 9.** Results of the initial (2021) and final (2023) measurements on the Ru-C cells at NPL. The two HTFP cells which circulated for thermodynamic temperature assignment are underlined.

Supplier	N	PL	VNI	NMIJ	
Cell ID	RU2002	RU2001	Ru-C6	Ru-C7	7ST-9
Initial inflection point (2021) (K)	2225.92	2226.44	2226.57	2226.5	2226.42
Final inflection point (2023) (K)	2226.12	2226.74	2226.64	2226.71	2226.7
Difference to T <sub>max</sub> (2023) (mK)	-620	0	-100	-30	-40
Drift (2023-2021) (mK)	0 (ref)	100	-130	10	80
Plateau shape	Good	Good	Very Good	Very Good	Good

The drifts inferred from these measurements were + 130 mK for the cell Ru-C6 and - 100 mK for the cell RU2001. These two cells remained the best two cells of the comparisons (initial and final) but not in the same positions. Moreover, the temperature measurement uncertainty, 400 mK (k=2) is larger than the total drift. Therefore, no correction was applied for the drift of the cells but an additional standard uncertainty of 66 mK (230 mK /  $2\sqrt{3}$ ; 230 mK being the difference between the measured drifts of the two selected cells) is added to the final thermodynamic temperature uncertainty.

# WC-C fixed point

The final comparison of WC-C HTFP cells was performed by LNE-Cnam, as per the initial comparison, using the same means and protocol as the initial comparison (relative temperatures using the pyrometer LP5 whose stability was daily monitored at the copper point), but it only concerned the two cells which circulated for thermodynamic temperature assignment: 7WC-C3 and 7WC-C5. The measurements were performed with each cell installed in the HTBB 3200-PG furnace and the temperature was measured relative to the highest fixed-point temperature, the cell 7WC-C5. The difference between the two cells was 52 mK in the initial stage and -11 mK at the final stage. The cells were remarkably stable. No correction for drift was applied and a standard uncertainty of 18 mK (63 mK /  $2\sqrt{3}$ ; 63 mK being the maximum measured difference between the two cells) was added to account for the stability of the cells.

#### THERMODYNAMIC TEMPERATURE ASSIGNMENT

The results of the thermodynamic temperatures reported by the six participating laboratories and the corresponding uncertainties are given in table 10 both for the POI and for the liquidus point.

Figures 1 and 2 show graphically the results of the measurements performed by the six participants. The agreement between the different determinations of the thermodynamic temperatures of the circulating HTFP cells is remarkable.

**TABLE 10.** Reported values of thermodynamic temperatures of the phase transitions of the HTFP at the POI and the liquidus point (corrected for emissivity and temperature drop). Uncertainties are those declared by each participant (k=2)

	Fe-C	U (Fe-C)	Pd-C	U (Pd-C)	Ru-C	U (Ru-C)	WC-C	U(WC-C)
Temperatures and uncertainties at the point of inflection of the melting plateau (K)								
LNE-Cnam	1426.69	0.21	1765.06	0.27	2227.01	0.39	3020.94	0.73
CEM	1426.69	0.23	1765.39	0.34	2227.35	0.54	3020.80	1.01
NIM	1426.78	0.17	1765.07	0.34	2226.98	0.49	3020.57	0.80
NPL	1426.76	0.11	1764.96	0.21	2227.07	0.40	3021.08	1.03
UME	1426.74	0.18	1764.99	0.36	2226.74	0.50	3020.53	1.17
PTB	1426.38	0.25	1764.93	0.45	2226.75	0.54	3021.13	0.95
			Temperatu	res and uncer	rtainties liqui	dus point (K)		
LNE-Cnam	1427.03	0.21	1765.30	0.27	2227.17	0.39	3021.02	0.73
CEM	1426.78	0.23	1765.43	0.34	2227.38	0.54	3020.86	1.01
NIM	1426.90	0.17	1765.17	0.34	2227.08	0.49	3020.62	0.80
NPL	1426.84	0.11	1765.06	0.23	2227.11	0.40	3021.21	1.06
UME	1426.84	0.18	1765.17	0.36	2226.79	0.50	3020.63	1.17
PTB	1426.71	0.25	1765.05	0.46	2226.80	0.54	3021.21	0.95

For all the HTFPs, except Fe-C, the differences between the two circulating HTFP cells were minor and no correction for drift was applied. However, an additional uncertainty component was added to account for the thermal effects and the instability of the cells.

The results of phase transition temperature assignment both for the POI and at the liquidus point are given in the table 11. The average values were derived from the six contributions using the uncertainty-weighted mean calculation as follows.

The weight,  $w_i$  given by

$$w_i = \frac{\frac{1}{u_i^2}}{\sum_{j=1}^{n} \frac{1}{u_j^2}} \tag{1}$$

the uncertainty-weighted average temperature  $\bar{T}$  would be:

$$\bar{T} = \sum_{i=1}^{n} w_i T_i \tag{2}$$

where  $T_i$  and  $u_i$  are values of the POI or liquidus point temperature and the standard uncertainty reported by the participant i among the n participants (n = 6 in our case).

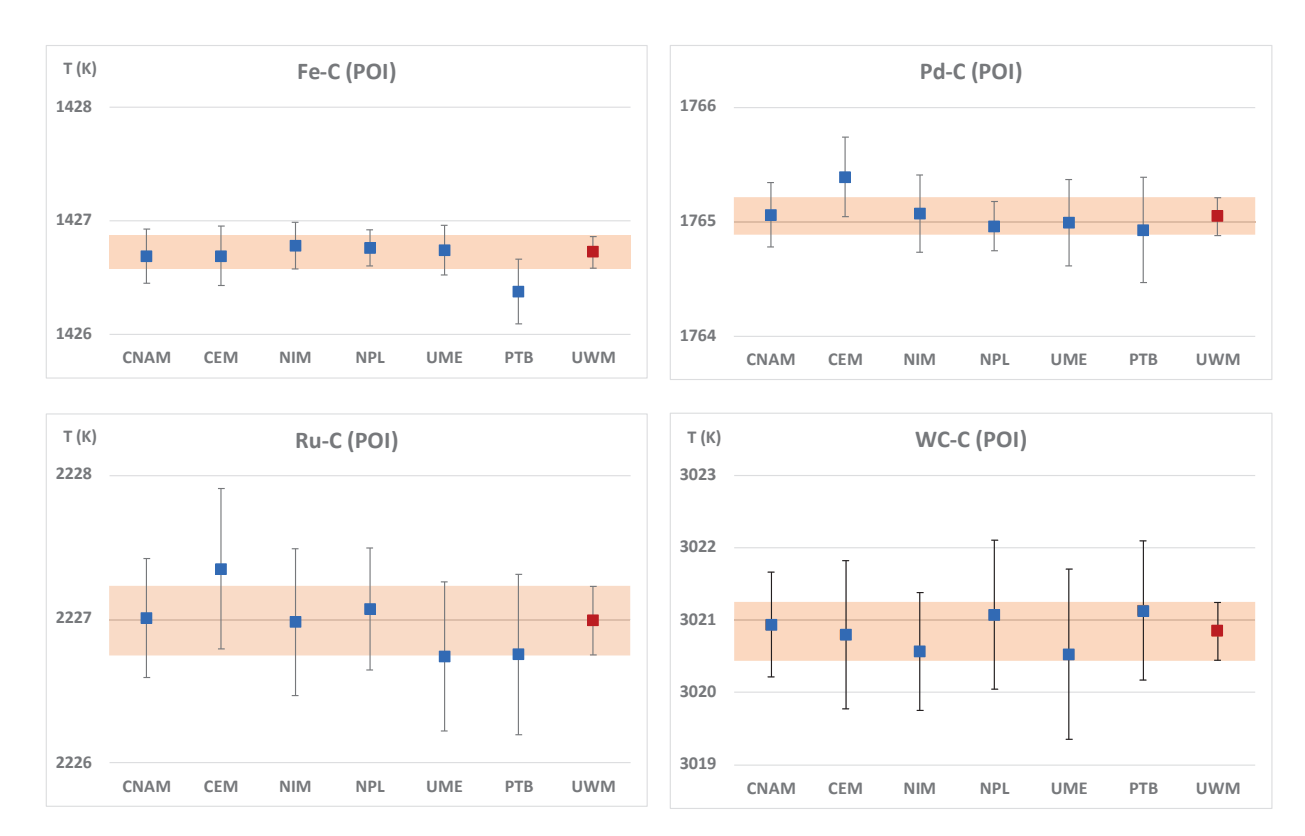


FIGURE 1. The final results as reported by the participants for the four HTFPs for the POI showing a good level of agreement between the independent measurements of the thermodynamic temperature. Uncertainties for the uncertainty-weighted mean (UWM) include uncertainty related to the thermal effect and the uncertainty on the stability of the cells. Uncertainty bars represent expanded uncertainties (k=2)

The weighted mean uncertainty is calculated from equation (2):

$$u_{\overline{T}}^2 = \sum_{i=1}^n \left(\frac{\partial \overline{T}}{\partial T_i}\right)^2 u_i^2 + 2\sum_{i=1}^{n-1} \sum_{j=i+1}^n \frac{\partial \overline{T}}{\partial T_i} \frac{\partial \overline{T}}{\partial T_j} r_{i,j} u_i u_j$$
(3)

Where  $u_i$  is the standard uncertainty submitted by laboratory i and  $r_{i,j}$  is the correlation coefficient between the uncertainties  $u_i$  and  $u_j$ . The determinations of T by the different participants were performed independently and therefore the correlation coefficient is considered null in equation (3).

The uncertainty on the uncertainty-weighted mean (UWM) value can therefore be derived as follows:

$$u_T^2 = \sum_{i=1}^n \left(\frac{\partial \bar{T}}{\partial T_i}\right)^2 u_i^2 = \sum_{i=1}^n w_i^2 u_i^2 = \frac{1}{\sum_{i=1}^n 1/u_i^2}$$
(4)

The final uncertainties account for this uncertainty on the mean weighted value as well as the stability of the cells and the thermal effect standard uncertainties estimated to be 25 mK for Fe-C, 50 mK for Pd-C, 30 mK for Ru-C and 75 mK for WC-C [11].

The uncertainty for the determination of the liquidus point temperature was derived from the uncertainty on the determination of the POI and the difference between the POI and the liquidus temperature.

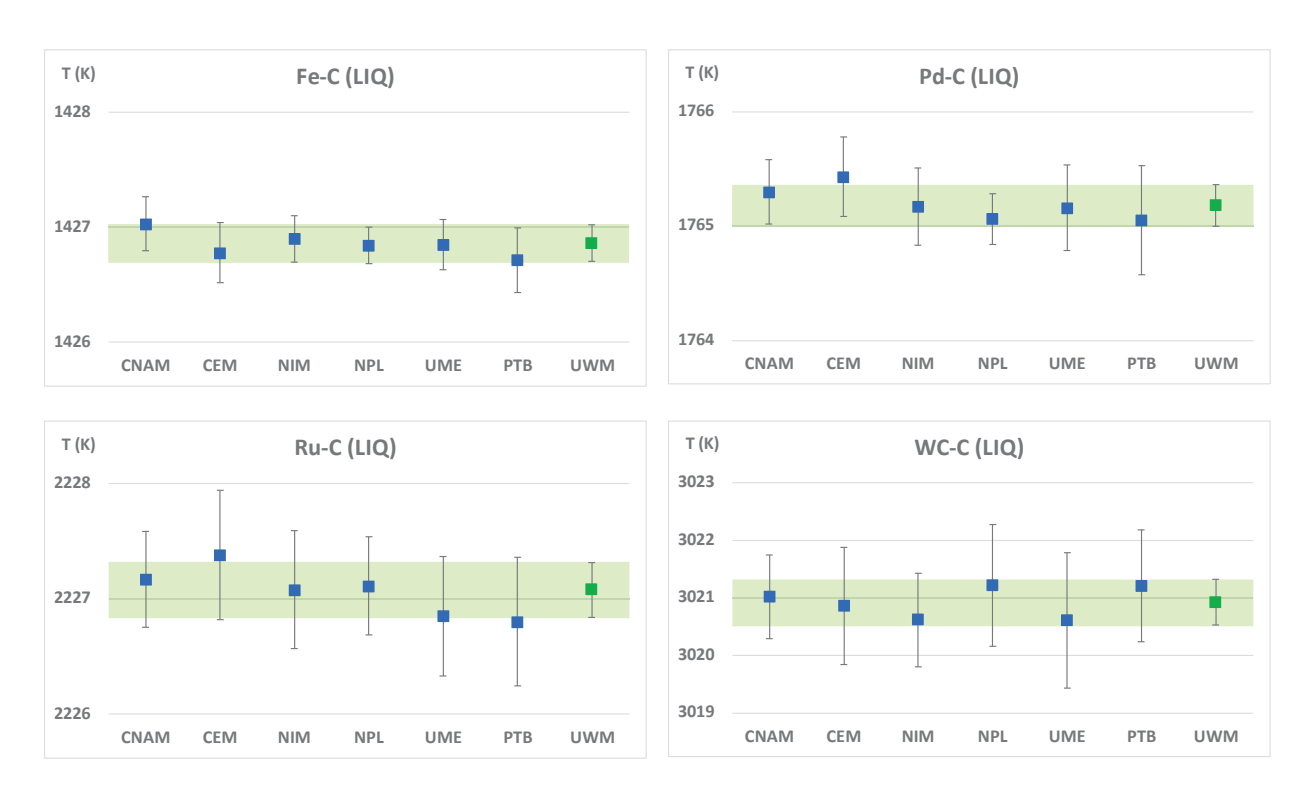


FIGURE 2. The final results as reported by the participants at the four HTFPs for the liquidus point. Uncertainties for the UWM include the thermal effect, the stability of the cells and the uncertainty on the determination of the liquidus temperature.

Uncertainty bars represent expanded uncertainties (*k*=2)

**TABLE 11.** Assigned thermodynamic temperature values for the POI and the liquidus point. Uncertainties include the uncertainties of the participants, the thermal effects, and an uncertainty component for the stability of the cells. The value at Fe-C was corrected as described above. The uncertainties  $U(T_{POI})$  and  $U(T_{LIQ})$  are expressed with a coverage factor k=2.

HTFP	$T_{POI}(K)$	$U(T_{POI})$ (K)	$T_{LIQ}(K)$	$U(T_{LIQ})$ (K)
Fe-C	1426.92	0.14	1427.02	0.16
Pd-C	1765.05	0.16	1765.18	0.18
Ru-C	2226.99	0.24	2227.08	0.24
WC-C	3020.85	0.40	3020.92	0.40

It is worth noticing that an excellent agreement between the participants was obtained during this collective thermodynamic temperature assignment work and that the uncertainties of the participants were quite homogeneous. Indeed, the differences between the mean values and the uncertainty-weighted values were very small and never exceeded 20 mK.

#### CONCLUSION

This work has made a major step forward for the *Mise-en-Pratique* of the kelvin at high temperatures by assigning low-uncertainty thermodynamic temperature values to a set of four high-temperature fixed points ranging from 1426 K to 3020 K. It completes the work begun during the European joint-research project "InK" [6, 7] and, when combined with those results<sup>2</sup>, allows the use of a total of seven high-temperature fixed points for the realisation of a practical thermodynamic temperature in agreement with the relative primary radiometry approach detailed in the *Mise-en-Pratique* of the kelvin [9, 21].

Finally, it is important to note that the final uncertainty budget of any thermodynamic temperature derived from this approach must include the in-use uncertainties as stated in the CCT task group on uncertainties of HTFPs [8].

#### **ACKNOWLEDGEMENT**

This paper has been written through fundings received from the EU EMPIR Programme co-financed by the Participating States and from the European Union's Horizon 2020 research and innovation programme, specifically from the EMPIR project 18SIB02 "Realising the redefined Kelvin".

#### REFERENCES

- 1. Anhalt K, Hartmann J, Lowe D, Machin G, Sadli M, Yamada Y. 2006 Thermodynamic temperature determinations of Co–C, Pd–C, Pt–C and Ru–C eutectic fixed-point cells. Metrologia 43, S78–S83. (https://doi.org/10.1088/0026-1394/43/2/S16)
- 2. Machin, G., 2013 Twelve years of high temperature fixed point research: A review, AIP Conference Proceedings 1552, 305 (2013); https://doi.org/10.1063/1.4821383
- Bourson F, Briaudeau S, Rougié B, Sadli M 2013 Determination of the Furnace Effect of Two High-Temperature Furnaces on Metal-Carbon Eutectic Points AIP Conference Proceedings 1552:380-5 https://doi.org/10.1063/1.4821389
- 4. Sadli, M., Pehlivan, O., Bourson, F., Diril, A., Ozcan, K., Collaboration Between UME and LNE-INM on Co-C Eutectic Fixed-Point Construction and Characterization Int. J. Thermophys., 30, 2009, pp. 36-46
- 5. Machin, G., et al., Measurement 94, p149–156 (2016).
- 6. Lowe D., et al. "The equilibrium liquidus temperatures of rhenium-carbon, platinum-carbon and cobalt-carbon eutectic alloys" Metrologia **54** 390-398 (2017). https://doi.org/10.1088/1681-7575/aa6eeb
- 7. Woolliams E et al "Thermodynamic temperature assignment to the point of inflection of the melting curve of high temperature fixed points" Phil. Trans. R. Soc. A **374** 20150044 (2016).
- 8. Todd A.D.W., Anhalt K., Bloembergen P., Khlevnoy B.B., Lowe D.H., Machin G., Sadli M., Sasajima N. and Saunders P. "On the uncertainties in the realization of the kelvin based on thermodynamic temperatures of high-temperature fixed-point cells" Metrologia **58** 035007 (2021).
- 9. Consultative Committee for Thermometry "The Mise-en-Pratique of the definition of the kelvin in the SI" SI Brochure 9<sup>th</sup> Edition (2019) Appendix 2 (<a href="https://www.bipm.org/documents/20126/41489682/SI-App2-kelvin.pdf/cd36cb68-3f00-05fd-339e-452df0b6215e">https://www.bipm.org/documents/20126/41489682/SI-App2-kelvin.pdf/cd36cb68-3f00-05fd-339e-452df0b6215e</a>)
- 10. Machin G., et al., Measurement 201, 111725 (2022).
- 11. Lowe D., Bourson F., Florio M., Girard F., Machin G., Mantilla J., Martin M.J., Nasibli H., Pehlivan Ö and Sadli M. "High-Temperature Fixed-Point Furnace Uncertainty" Proceedings of the 10th International Temperature Symposium (ITS10), in press.
- 12. Anhalt K., et al "Dissemination of thermodynamic temperature using of Fe-C and Pd-C high-temperature fixed point cells" High Temperatures High Pressures, to be published, 2023.

 $<sup>^2</sup>$  Thermodynamic temperature values assigned to Co-C, Pt-C and Re-C in [6,7] are (exp. uncertainties, k=2):  $T_{LIQ}(\text{Co-C}) = 1597.476~\text{K} \pm 0.142~\text{K}; T_{LIQ}(\text{Pt-C}) = 2011.502~\text{K} \pm 0.220~\text{K}; T_{LIQ}(\text{Re-C}) = 2747.909~\text{K} \pm 0.440~\text{K}.$   $T_{POI}(\text{Co-C}) = 1597.39~\text{K} \pm 0.13~\text{K}; T_{POI}(\text{Pt-C}) = 2011.43~\text{K} \pm 0.18~\text{K}; T_{POI}(\text{Re-C}) = 2747.84~\text{K} \pm 0.35~\text{K}.$ 

- 13. Bourson F., Briaudeau S., Rougié B., Sadli M., Acta Metrol. Sin. 29, 1 (2008).
- 14. Martin M.J., Mantilla J.M., del Campo D., Herranz M.L., Pons A. and Campos J. "Performance of different light sources for the absolute calibration of radiation thermometers" Int J Thermophys 38, 138, (2017).
- 15. Martín M.J., Mantilla J.M., Garcia-Izquierdo C., del Campo D. "Construction, Characterization and Measurement of Fe–C and Pd–C HTFPs at CEM" Int J Thermophys **43**, 57 (2022). https://doi.org/10.1007/s10765-022-02978-2
- 16. Anhalt K., Hartmann J., Lowe D., Machin G., Sadli M., Yamada Y., "Thermodynamic temperature determinations of Co–C, Pd–C, Pt–C and Ru–C eutectic fixed-point cells" Metrologia 43, S78–S83 (2006).
- 17. Machin, G., Anhalt, K., Bloembergen, P., Sadli, M., Lowe, D., Saunders, P., Yamada, Y., Yoon H., "MEP-K Relative Primary Radiometric Thermometry" Edition 2017 BIPM website
- 18. Salim S G R, Briaudeau S, Bourson F, Rougié B, Truong D, Kozlova O, Coutin J-M and Sadli M, "A reference radiance-meter system for thermodynamic temperature measurements" Metrologia **53**, 945 (2016).
- 19. Bourson F., et al "Realisation of the ITS-90 and thermodynamic temperature measurements above 960 °C using a monochromator-based radiance comparator", Metrologia **59** 015003 (2022).
- 20. Bloembergen P., Yamada Y., Sasajima N., Wang Y. and Wang T. "The effect of the eutectic structure and the residual effect of impurities on the uncertainty in the eutectic temperatures of Fe–C and Co–C" Metrologia 44, 279–293 (2007).
- 21. Lowe, D., and Machin, G., "Low uncertainty thermodynamic temperature measurement using relative primary radiometry Setting up n=2 scale using copper and rhenium-carbon with uncertainties", ITS-10 In Press (2023).